Analytical Development of a Robust Controller for Smart Structural Systems

Chul Hue Park*, Seong Il Hong, Hyun Chul Park
Department of Mechanical Engineering,
Pohang University of Science and Technology (POSTECH),
Pohang, KyungBuk 790-784, Korea

This paper aims at demonstrating the feasibility of active control of beams with a multiobjective state-feedback control technique. The multiobjective state-feedback controller is designed on a linear matrix inequality (LMI) approach for the multiobjective synthesis. The design objectives are to achieve a mix of H_∞ performance and H_2 performance satisfying constraints on the closed-loop pole locations in the face of model uncertainties. The controller is also designed to reject the effects of the noise and external of disturbances. For the theoretical analysis, the governing equation of motion is derived by Hamilton's principle to describe the dynamics of a smart structural system. Numerical examples are presented to demonstrate the effectiveness of the integrated robust controller in damping out the multiple vibration modes of the piezo/beam system.

Key Words : Linear Matrix Inequality, Multiobjective State-feedback Control, Robust Control, Smart Structure System

1. Introduction

As system elements become more lightweight, to satisfy inertia and size requirement, vibration becomes a dominant factor in their undesirable dynamic behavior. The unwanted vibration problem could be avoided through the use of active layer damping treatments. In the simplest form of active layer damping system, two piezoelectric ceramics are bonded symmetrically to a vibrating structure and have abilities of producing and/or monitoring structural deformations. Active vibration control scheme has been heavily researched in the past decade because of their high power density as compared with conventional actuators. Especially, the real time sensing and actuation capabilities provide a powerful means for active vibration control.

Bailey and Hubbard (1985) proposed to use a piezoelectric polymer as a distributed parameter actuator and designed an active vibration damper using a distributed parameter theory. Lyapunov's second method for distributed- parameter systems was used to design a control algorithm for the active damper. Fanson and Caughey (1990) introduced PPF (Positive Position Feedback) for vibration suppression in large space structure which is investigated in laboratory experiments on a thin cantilever beam. This technique makes use of generalized displacement measurements to accomplish vibration reduction. Kim and Nam (1996) designed an active flutter suppression system of a composite plate wing model using a reduced order model. The control parameters were determined using the mixed-sensitivity H_∞ control method. Shin et al.(1998) presented the active vibration control of a flexible cantilever beam by adopting the adaptive controller based on the Filtered-X LMS algorithm.

* Corresponding Author,
E-mail : drparkch@postech.ac.kr
TEL : +82-54-279-2962; **FAX** : +82-54-279-5899
Department of Mechanical Engineering, Pohang University of Science and Technology San 31 Hyoja Dong, Pohang, KyungBuk 790-784, Korea. (Manuscript **Received** November 17, 2004; **Revised** March 25, 2005)

In this paper, the feasibility of active layer damping for beams is investigated by using a multiobjective state-feedback control technique. The multiobjective control law is designed as considering the fact that the closed-loop system satisfies a number of objectives such as disturbance attenuation to achieve the wanted performance in time and frequency domain and robust stabilization of uncertain system. For frequency domain performance, a mixed H_2/H_∞ controller is adopted (Bernstein and Haddad, 1989). This approach is to minimize an auxiliary cost subject to an H_∞ norm constraint, and this cost yields an upper bound on the H_2 norm. In contrast to the mixed H_2/H_∞ control theory, regional pole placement constraints are added to offer a numerically tractable means of attacking problems in time domain. Satisfactory time response and closed-loop damping can be achieved by forcing the closed-loop poles into a suitable subregion of the left-half plane (Chilali and Gahinet, 1996). These constraints of mixed H_2/H_∞ synthesis and regional pole placement are expressed in terms of linear matrix inequalities (LMI). The global stability and applicability of an LMI based multiobjective state-feedback controller are presented by numerical simulations in damping out the multiple vibration modes of the piezo/beam system in the face of uncertainties, noise and external disturbances.

2. Equation of Motion of the Piezo/beam System

The mathematical model of a piezo/beam system is developed to describe the flexural vibration behavior of a cantilevered piezo/beam system. The schematic drawings of the proposed smart structure are illustrated in Fig. 1. The beam has length l_b, width b_b, thickness t_b, and mass density ρ_b. The PZT has thickness t_p, elastic modulus measured at constant electric field E_p, and piezoelectric constant d_{31} in the longitudinal direction. The derivation of system equations is based on the assumption of Euler Bernoulli beam. The constitutive equation for a piezoelectric element depends on the mechanical stress, σ, strain, ε,

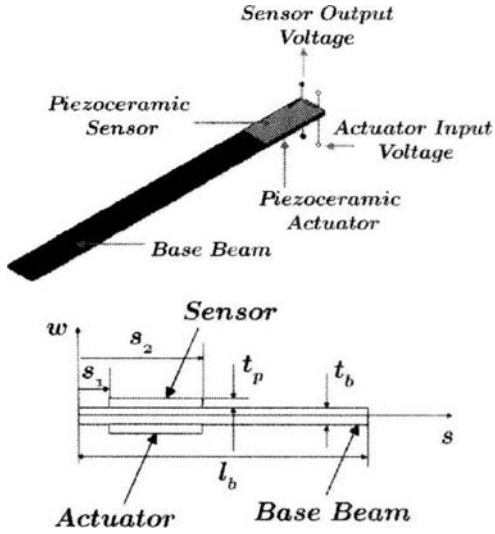

Fig. 1 Schematic drawings of smart structural system

as well as the electric field, E, and the electric displacement, D. The constitutive equation of the piezoelectric material can be written as (IEEE, 1987)

$$\begin{bmatrix}\sigma\\ E\end{bmatrix}=\begin{bmatrix}E_p & -h_{31}\\ -h_{31} & \beta_{33}\end{bmatrix}\begin{bmatrix}\varepsilon\\ D\end{bmatrix} \tag{1}$$

where E_p is the elastic modulus at the constant displacement, h_{31} is the piezoelectric constant, and β_{33} is the dielectric constant.

The kinetic energy of a piezo/beam system can be described as

$$T=T_b+2T_p \tag{2}$$

where $T_b=\frac{1}{2}\int_0^{l_b}\rho_b A_b\left(\frac{\partial w}{\partial t}\right)^2 ds$,

$$T_p=\frac{1}{2}\int_0^{l_b}\rho_b A_p\left(\frac{\partial w}{\partial t}\right)^2[H(s-s_1)-H(s-s_2)]\,ds.$$

Here, T_b and T_p are the kinetic energy of a base beam and piezoceramic layer, respectively. H is the Heaviside's function, w is the transverse displacement of the beam, and A_b, A_p are the cross sectional area of beam and piezo layer, respectively. The subscripts b and p represent the base beam and piezoceramic, respectively. It is noted that there are two piezoceramics in the piezo/beam system as shown in Fig. 1: one is attached on the beam as a sensor (denoted by subscript s), the other is beneath the beam as an actuator (denoted by subscript a).

The strain energy of a piezo/beam system can be described as

$$U=U_b+U_s+U_a \tag{3}$$

where

$$U_b=\frac{1}{2}\int_0^{l_b}E_bI_b\left(\frac{\partial^2 w}{\partial s^2}\right)^2 ds$$

$$U_a=\frac{1}{2}\int_V(\varepsilon\sigma+E_aD_a)\,dV$$
$$=\frac{1}{2}\int_0^{l_b}\left[E_pI_p\left(\frac{\partial^2 w}{\partial s^2}\right)^2+2A_ph_{31}D_az_n\left(\frac{\partial^2 w}{\partial s^2}\right)+A_p\beta_{33}D_a^2\right][H(s-s_1)-H(s-s_2)\,ds]$$

$$U_s=\frac{1}{2}\int_V\varepsilon\sigma dV$$
$$=\frac{1}{2}\int_0^{l_b}\left[E_pI_p\left(\frac{\partial^2 w}{\partial s^2}\right)^2\right][H(s-s_1)-H(s-s_2)]\,ds$$

Here, $z_n=\frac{1}{2}(t_b+t_p)$ and I_b and I_p are the area moment of inertia about the neutral axis of the each layer. Moreover, D_a represents the electric displacement of the piezo sensing and actuating layer, respectively.

The virtual work consists of two terms : the first term is the work done by external force, and the second is the inherent damping force of a base structure.

$$\delta W=\int_0^{l_b}f(s,\,t)\,\delta w ds-\int_0^{l_b}c_b\frac{\partial w}{\partial t}\,\delta w ds \tag{4}$$

The equations of motion can be obtained by applying Hamilton's principle (Meirovitch, 1967)

$$\delta H=\delta\int_{t_1}^{t_2}(T-U+W)\,dt=0 \tag{5}$$

where t_1 and t_2 are the end of points in the time domain and δ is the variational operator. Substituting the potential energy, kinetic energy, and virtual work into Hamilton's principle yields the following equations of motion.

$$\rho_bA_b\left(\frac{\partial^2 w}{\partial t^2}\right)+c_b\left(\frac{\partial w}{\partial t}\right)+E_bI_b\left(\frac{\partial^4 w}{\partial s^4}\right)$$
$$+2\left[\rho_pA_p\left(\frac{\partial^2 w}{\partial t^2}\right)+E_pI_p\left(\frac{\partial^4 w}{\partial s^4}\right)\right][H(s-s_1)-H(s-s_2)] \tag{6}$$
$$=f(s,\,t)-\frac{1}{2}b_ph_{31}D_at_p(t_b+t_p)\left(\frac{\partial^2}{\partial s^2}[H(s-s_1)-H(s-s_2)]\right)$$

where b_p is the width of the piezoceramic. The assumed mode method is used to discretize the governing equation [Eq. (6)] into a set of ordinary differential equation. The flexural motion for a cantilever beam is approximated by

$$w(s,\,t)=\sum_{i=1}^{\infty}\psi_i(s)\,\eta_i(t) \tag{7}$$

where $\psi_i(s)=\sin\beta_is-\sinh\beta_is-\alpha_i(\cosh\beta_is-\cos\beta_is)$. Here the constants $\alpha_i=(\sin\beta_il_b+\sinh\beta_il_b)/(\cos\beta_il_b+\cosh\beta_il_b)$ are the mode shape coefficients (Rao, 1995). Applying mode shape functions to the equation of motion [Eq. (6)] results in the following discretized differential equations of the piezo/beam system.

$$M_i\ddot{\eta}_i(t)+H_i\dot{\eta}_i(t)+K_i\eta_i(t)=f_{i,ext}+f_{i,piezo},\quad i=1,\,2,\,\cdots,\,\infty \tag{8}$$

where

$$M_i=\rho_bA_b\int_0^{l_b}\psi_i(s)^2ds$$
$$+2\rho_pA_b\int_0^{l_b}\psi_i(s)^2[H(s-s_1)-H(s-s_2)]\,ds$$

$$C_i=c_b\int_0^{l_b}\psi_i'(s)^2ds$$

$$K_i=E_bI_b\int_0^{l_b}\psi_i''(s)^2ds$$
$$+2E_pI_p\int_0^{l_b}\psi_i''(s)^2[H(s-s_1)-H(s-s_2)]\,ds$$

$$f_{i,ext}=\int_0^{l_b}\psi_i(s)\,f(s,\,t)\,ds$$

$$f_{i,piezo}=-\frac{1}{2}b_pd_{31}E_pV_c(t)\,(t_b+t_p)$$
$$\times\int_0^{l_b}\psi_i(s)\,[\delta'(s-s_1)-\delta'(s-s_2)]\,ds$$

where $V_c(t)$ is the actuator input voltage and d_{31} is the piezoelectric material constant.

The charge generated by the piezo sensor layer is related to the bending strain of the cantilever beam as follows (Pota and Alberts, 1995) :

$$q(s,\,t)=\left(\frac{k_{31}^2}{g_{31}}\right)\varepsilon_c(s,\,t)\,b_p \tag{9}$$

where k_{31} is the electromechanical coupling constant ; g_{31} is the piezoelectric stress constant ; and ε_c is the bending strain of the system. The total charge developed on the sensing layer is obtained

by integrating $q(s, t)$ over the entire length of the piezoelectric element,

$$Q(t)=\int_0^{l_b} q(s, t)[H(s-s_1)-H(s-s_2)]ds$$
$$=\int_0^{l_b} b_p\left(\frac{t_b}{2}+t_p\right)\frac{k_{31}^2}{g_{31}}\frac{\partial^2 w}{\partial s^2}[H(s-s_1)-H(s-s_2)]ds \quad (10)$$

Applying mode shape functions, the sensor voltage is given by the following formula

$$V_s(t)=\frac{Q(t)}{Cb_p(s_2-s_1)}$$
$$=\frac{1}{C(s_2-s_1)}\sum_{i=0}^{\infty}\left[\int_0^{l_b}\left(\frac{t_b}{2}+t_p\right)\frac{k_{31}^2}{g_{31}}\frac{\partial^2\psi_i(s)}{\partial s^2}\right. \quad (11)$$
$$\left.\times[H(s-s_1)-H(s-s_2)]ds\right]\eta_i(t),$$
$$i=1, 2, \cdots, \infty$$

where C is the capacitance per unit area and $b_p(s_2-s_1)$ is the surface area of the piezoelectric element.

3. LMI Formulations of the System Performance

The governing equation [Eq. (8)] of the piezo/beam system can be transformed into the following modal differential equation.

$$\ddot{\eta}_i(t)+2\zeta_i\omega_i\dot{\eta}_i(t)+\omega_i^2\eta_i(t)$$
$$=\bar{f}_{iext}+\bar{f}_{i,piezo}, \quad i=1, 2, \cdots, \infty \quad (12)$$

where ω_i and ζ_i are the modal frequency and damping ratio of the i-th mode, respectively. The lowest n finite modes will be actively controlled and the remainder mode be classified as residual modes. The discretized structure modal equation [Eq. (12)] and output sensor equation [Eq. (11)] can be expressed in a standard state-space form as considering a linear time-invariant (LTI) system.

$$\begin{aligned}\dot{x}(t)&=Ax(t)+B_uu(t)+B_ww(t)\\ z_\infty(t)&=C_{\infty}x(t)+D_{\infty u}u(t)+D_{\infty w}w(t)\\ z_2(t)&=C_2x(t)+D_{2u}u(t)+D_{2w}w(t)\\ y(t)&=C_yx(t)+D_{yu}u(t)+D_{yw}w(t)\end{aligned} \quad (13)$$

where $x(t)=\Re_+\rightarrow\Re^n$, $u(t)$: $\Re_+\rightarrow\Re^{n_u}$, $w(t)$: $\Re_+\rightarrow\Re^{n_w}$, $z_\infty(t)$: $\Re_+\rightarrow\Re^{n_{z\infty}}$, $z_2(t)$: $\Re_+\rightarrow\Re^{n_{z2}}$ and $y(t)$: $\Re\rightarrow\Re^{n_y}$. The controlled mode state vectors are defined by $x(t)=[\eta_1(t), \eta_2(t), \cdots, \eta_m(t), \dot{\eta}_{m+1}(t), \cdots, \dot{\eta}_n(t)]\in\Re^n$. Moreover, $u(t)$ is the control input; $w(t)$ is the exogenous input; $z_\infty(t)$ and $z_2(t)$ are regulated output; and $y(t)$ is measured output. The specifications and objectives under consideration include H_∞ performance and H_2 performance. The standard H_2/H_∞ feedback configuration for the two linear time-invariant systems is shown in Fig. 2.

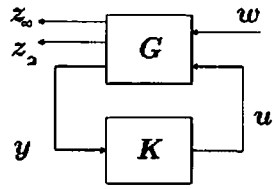

Fig. 2 Standard H_2/H_∞ feedback configuration

3.1 H_∞ performance

In this section, we construct a state-feedback controller which is arbitrarily close to the H_∞ optimum (Gahinet and Apkarian, 1994; Khargonekar et al., 1988; Petersen, 1987). Our objective is to find a static state feedback controller $u=Kx$ such that the resulting closed-loop transfer matrix has H_∞ norm smaller than some a priori given upper bound. Consider again the system (13). The closed-loop system can be described by

$$\begin{aligned}\dot{x}(t)&=A_{cl}x(t)+B_ww(t)\\ z_\infty(t)&=C_{cl}x(t)+D_{\infty w}w(t)\end{aligned} \quad (14)$$

where $A_{cl}=A+B_uK$ and $C_{cl}=C_\infty+D_{\infty u}K$.

Suppose there exists a quadratic Lyapunov function $V(t)=x^TPx$, $P>0$, and for any real number $\gamma\geq 0$ such that for all t (Boyd et al., 1994),

$$\frac{d}{dt}V(x(t))+z_\infty(t)^Tz_\infty(t)-\gamma^2w(t)^Tw(t)<0 \quad (15)$$

To show this, we integrate (15) from 0 to T, with the initial condition $x(0)=0$, to obtain

$$V(x(T))+\int_0^T[z_\infty(t)^Tz_\infty(t)-\gamma^2w(t)^Tw(t)]dt<0 \quad (16)$$

Since $V(x(T))\geq 0$, this implies

$$\frac{\| z_\infty(t) \|_2}{\| w(t) \|_2} < \gamma \tag{17}$$

From the Eq. (16), the closed-loop system yields the following conditions

$$\begin{bmatrix} AQ_\infty + Q_\infty A^T + B_u L + L^T B_u^T & B_w & Q_\infty C_\infty^T + L^T D_{\infty u}^T \\ B_w^T & -\gamma^2 I & D_{\infty w}^T \\ C_\infty Q_\infty + D_{\infty u} L & D_{\infty w} & -I \end{bmatrix} < 0,\ Q_\infty > 0 \tag{18}$$

where $Q_\infty = P_\infty^{-1}$. The optimal solution is computed by minimizing γ over the variables Q_∞, L and γ satisfying conditions (18).

3.2 H_2 performance

The H_2 state feedback control problem is to find a static control gain K that stabilizes system internally and minimizes the H_2 norm of the transfer matrix T_{wz} from $w(t)$ to $z_2(t)$. Let us introduce a short hand notation of the closed loop system as follows:

$$\begin{aligned} \dot{x}(t) &= A_{cl} x(t) + B_w w(t) \\ z_2(t) &= C_{cl2} x(t) \end{aligned} \tag{19}$$

where $A_{cl} = A + B_u K$ and $C_{cl2} = C_2 + D_{2u} K$. And recall that $\| T_{wz} \|_2^2 = trace(C_{cl2} Q_c C_{cl2}^T)$ where Q_c is the solution of the following *Lyapunov equation and controllability Gramian* (Scherer et al., 1997),

$$A_{cl} Q_c + Q_c A_{cl}^T + B_w B_w^T = 0 \tag{20}$$

Since $Q_c < Q_2$ for any symmetric $Q_2 > 0$, $\| T_{wz_2} \|_2^2 = trace(C_{cl2} Q_c C_{cl2}^T) < trace(C_{cl2} Q_2 C_{cl2}^T) < trace(Y)$ whenever the symmetric matrices Q_2 and Y satisfy

$$\begin{bmatrix} AQ_2 + Q_2 A^T + B_u L + L^T B_u^T & B_w \\ B_w^T & -I \end{bmatrix} < 0$$
$$\begin{bmatrix} Y & C_2 Q_2 + D_{2u} L \\ Q_2 C_2^T + L^T D_{2u}^T & Q_2 \end{bmatrix} < 0,\ Q_2 > 0 \tag{21}$$

where $L = K Q_2$. We can compute optimal solution by minimizing Y satisfying conditions (21).

3.3 Regional pole constraints

It is known that the transient response of a linear system is related to the locations of its poles (Ogata, 1990). Confining the closed-loop poles to this region as shown in Fig. 3 ensures a minimum decay rate α, a minimum damping ratio ζ, and a maximum undamped natural frequency ω_d. This fact makes LMI regions particularly appealing for synthesis purposes. Let the LMI region be characterized in terms of the $m \times m$ block matrix

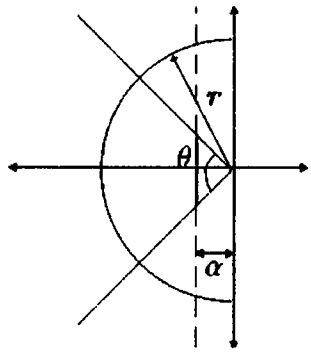

Fig. 3 Pole placement region

$$\begin{aligned} &M_{\mathfrak{R}}(A_{cl}, Q_R): \\ &= \alpha \otimes Q_R + \beta \otimes (A_{cl} Q_R) + \beta^T \otimes (A_{cl} Q_R)^T \\ &= [\alpha_{kl} Q_R + \beta_{kl} A_{cl} Q_R + \beta_{lk} Q_R A_{cl}^T]_{1 \le k,l \le m} \end{aligned} \tag{22}$$

The matrix A_{cl} is -stable if and only if there exists a symmetric matrix $Q_{\mathfrak{R}}$ such that (Chilali and Gahinet, 1996)

$$M_R(A_{cl}, Q_R) < 0,\ Q_R > 0 \tag{23}$$

It should be noted that for the class of LMI regions R_1 and R_2 and their associated characteristic functions f_{R_1} and f_{R_2}, the intersection $R = R_1 \cap R_2$ is also an LMI region.

4. Multiobjective Synthesis

In the previous section, several time-and frequency-domain specifications have been expressed as LMI constraints on the closed-loop state space matrices. These analysis results are now used for multiobjective synthesis. The objective of the synthesis is to minimize the H_2 norm of $\| T_{wz2} \|$ over all state-feedback gains K that enforce the H_∞ and pole placement constraints. From a previous discussion, this is equivalent to minimizing $trace(Y)$ over all matrices Q_∞, Q_2, Q_R, Y and L satisfying (18), (21), and (23). In order to recover convexity, all specifications are enforced by a single closed-loop Lyapunov function $V(x(t)) = x^T Q^{-1} x$ with $Q > 0$. This amounts

to imposing the constraint.

$$Q=Q_\infty=Q_2=Q_R \tag{24}$$

With (24) in force, all inequalities can be further reduced to linear matrix inequalities. Clearly, this restriction is stringent and brings conservatism into the design. Nevertheless, the resulting synthesis technique has valuable merits over existing alternatives (Scherer et al., 1997). The solution can be sought by substituting (24) to (18), (21), and (23). Admittedly with some conservatism, we are left with computing

$$J(T_{wz2}):=\inf\{trace(Y):\ Q,\ Y,\ L\ satisfy\ (18),\ (21)\ and\ (23)\ with\ Q=Q_\infty=Q_2=Q_R\} \tag{25}$$

The H_2 performance index $J(T_{wz_2})$ defined by (25) can be computed as the global minimum of the following LMI optimization problem.

Minimize $trace(Y)$ *over* $Q=Q^T>0$, $Y=Y^T$ *and* L *subject to the LMI constraints.*

$$\begin{bmatrix} AQ+QA^T+B_uL+L^TB_u^T & B_w & QC_\infty^T+L^TD_{\infty u}^T \\ B_w^T & -\gamma^2 I & D_{\infty w}^T \\ C_\infty Q+D_{\infty u}L & D_{\infty w} & -I \end{bmatrix}<0$$

$$\begin{bmatrix} Y & C_2Q+D_{2u}L \\ QC_2^T+L^TD_{2u}^T & Q \end{bmatrix}<0 \tag{26}$$

$$[\alpha_{kl}Q+B_{kl}(AQ+B_uL)+\beta_{lk}(QA^T+L^TB_u^T)]_{1\le k,l\le m}<0$$

The auxiliary performance $J(T_{wz_2})$ is an upper estimate of the optimal H_2 performance subject to the H_∞ and pole placement constraints.

5. Uncertainty

The parameter uncertainties for this study are ±4% range of natural frequency variations at the first mode. These uncertainties are modeled by affine parameter dependent uncertainties and then transformed into polytopic state-space model (Boyd et al., 1994). Following explanation can be extended to entire uncertain system.

5.1 Affine parameter dependent models (PDS)

The dynamic equations of motions with uncertain coefficients give rise to parameter dependent models of the form

$$\begin{aligned} &\dot{x}(t)=A(p)x(t)+B_uu(t)\\ &\text{with } A(p)=A_0+p_1A_1+\cdots+p_nA_n \end{aligned} \tag{27}$$

where $A(\cdot)$ are known functions of some parameter vector $p=p(p_1, \cdots, p_n)$. The coefficients, $A_o, \cdots, A_n$, fully characterize the dependence on the uncertain parameters, $p_1, \cdots, p_n$. Parameter uncertainty is quantified by the range of parameter values and possibly the rates of parameter variation. The parameter uncertainty range can be described as a box in the parameter space. In other words, p_i ranges between two empirically determined extremal values $p_i\in[\underline{p_i}, \overline{p_i}]$.

5.2 Polytopic models

We call polytopic system a linear time-varying system

$$\dot{x}(t)=A(t)x(t)+B_uu(t) \tag{28}$$

whose $A(t)$ matrix varies within a fixed polytope of matrices, i.e.,

$$\begin{aligned} &A(t)\in Co\{A_1, \cdots, A_N\}:\\ &=\left\{\sum_{i=1}^N q_iA_i:\ q_i\ge 0,\ \sum_{i=1}^N q_i=1\right\} \end{aligned} \tag{29}$$

where $A_1, \cdots, A_N$ are given vertex systems and "Co" means the convex hull. In other words, $A(t)$ is a convex combination of the matrices $A_1, \cdots, A_N$. The nonnegative number $q_1, \cdots, q_n$ are called the polytopic coordnates of A. Affine parameter-dependent models are converted to polytopic ones. The parameter vector $p=p(p_1, \cdots, p_n)$ takes values in a parameter box with 2^n corners. If the function $A(p)$ is affine in p, it maps this parameter box to some polytope of A matrices.

5.3 Extension to uncertain systems

The closed-loop systems discussed above are extended to uncertain system described by a polytopic state-space model. Seeking a single quadratic Lyapunov function that enforces the design objectives for all plants in the polytope leads to the following multi-model counterpart of the LMI conditions.

Minimize trace (Y) *over* $Q=Q^T\geq 0$, $Y=Y^T$ *and* L *subject to the LMI constraints.*

$$\begin{bmatrix} A_iQ+QA_i^T+B_uL+L^TB_u^T & B_w & QC_\infty^T+L^TD_{\infty u}^T \\ B_w^T & -\gamma^2 I & D_{\infty w}^T \\ C_\infty Q+D_{\infty u}L & D_{\infty w} & -I \end{bmatrix}<0$$

$$\begin{bmatrix} Y & C_2Q+D_{2u}L \\ QC_2^T+L^TD_{2u}^T & Q \end{bmatrix}<0 \qquad (30)$$

$$[a_{kl}Q+\beta_{kl}(A_iQ+B_uL)+\beta_{lk}(QA_i^T+L^TB_u^T)]_{1\leq k,l\leq m}<0,$$
$$i=1,\cdots,N$$

where $Q=P^{-1}$ and $L=KQ$. We compute optimal solution by minimizing γ over the variables Q, L and γ satisfying the above conditions.

6. Numerical Analysis

To illustrate the effectiveness of the multiobjective state-feedback controller in suppressing the multi-mode vibration control of the piezo/beam system, numerical analysis is performed with the help of MATLAB Toolbox (Gahinet et al., 1995). The physical and geometrical parameters of the aluminum beam and PZT are indicated in Tables 1 and 2. The inherent modal damping ratio ζ of the piezo/beam system is assumed by 0.002 for the each mode.

Table 1 Physical and geometrical parameters of aluminum beam

Property	Symbol	Value
Young's modulus	E_b	69×10^9 Pa
Beam density	ρ_b	2700 kg/m^3
Beam width	b_b	20.7 mm
Beam thickness	t_b	2 mm
Beam length	l_b	250 mm

Table 2 Physical and geometrical parameters of PZT

Property	Symbol	Value
Young's modulus	E_p	5.9×10^9 Pa
PZT density	ρ_p	7800 kg/m^3
PZT width	b_p	20 7 mm
PZT thickness	t_p	0.267 mm
PZT charge constant	d_{31}	-260×10^{-12} (C/N)
Coupling coefficient	k_{31}	0.36
PZT voltage constant	g_{31}	9.5×10^{-3} (m^2/C)
End point of PZT	s_2	5.1 cm
Start point of PZT	s_1	0.1 cm

The state-space model of the overall augmented piezoelectric laminated beam system is given by

$$\Sigma:\begin{cases} \dot{x}(t)=Ax(t)+B_uu(t)+B_ww(t) \\ z_\infty(t)=C_\infty x(t)+D_{\infty u}u(t)+D_{\infty w}w(t) \\ z_2(t)=C_2x(t)+D_{2u}u(t)+D_{2w}w(t) \\ y(t)=C_yx(t)+D_{yu}u(t)+D_{yw}w(t) \end{cases} \qquad (31)$$

with

$$A=\begin{bmatrix} 0 & 0 & 0 & 1 & 0 & 0 \\ 0 & 0 & 0 & 0 & 1 & 0 \\ 0 & 0 & 0 & 0 & 0 & 1 \\ -\omega_1^2 & 0 & 0 & -2\zeta_1\omega_1 & 0 & 0 \\ 0 & -\omega_2^2 & 0 & 0 & -2\zeta_2\omega_2 & 0 \\ 0 & 0 & -\omega_3^2 & 0 & 0 & -2\zeta_3\omega_3 \end{bmatrix}$$

$$=\begin{bmatrix} 0 & 0 & 0 & 1 & 0 & 0 \\ 0 & 0 & 0 & 0 & 1 & 0 \\ 0 & 0 & 0 & 0 & 0 & 1 \\ -38887 & 0 & 0 & -0.8 & 0 & 0 \\ 0 & -1318674 & 0 & 0 & -4.6 & 0 \\ 0 & 0 & -9424900 & 0 & 0 & -12.3 \end{bmatrix}$$

$$B_u=\begin{bmatrix} 0 \\ 0 \\ 0 \\ 6.206 \\ 2.278 \\ 2.680 \end{bmatrix},\ B_w=\begin{bmatrix} 0 \\ 0 \\ 0 \\ 71.530 \\ -70.620 \\ 67\,298 \end{bmatrix},\ C_\infty=\begin{bmatrix} 1.323 \\ 4.920 \\ 6.090 \\ 0 \\ 0 \\ 0 \end{bmatrix}$$

$$C_2=\begin{bmatrix} 1\,3236 & 0 & 0 & 0\,0\,0 \\ 0 & 4.921 & 0 & 0\,0\,0 \\ 0 & 0 & 6.090 & 0\,0\,0 \\ 0 & 0 & 0 & 1\,0\,0 \\ 0 & 0 & 0 & 0\,1\,0 \\ 0 & 0 & 0 & 0\,0\,1 \end{bmatrix},\ D_{2u}=\begin{bmatrix} 0 \\ 0 \\ 0 \\ 3.103 \\ 1.140 \\ 1.345 \end{bmatrix}$$

$$D_{\infty u}=D_{\infty w}=D_{2w}=D_{yu}=D_{yw}=0,\ C_y=I$$

Control objectives are as follows:

(1) Guarantee stability of closed-loop system and to minimize the influence of the disturbance.

(2) Obtain good trade-off between the H_∞ performance and H_2 performance.

Minimize $\|T_{wz_2}\|_2$ *subject to* $\|T_{wz_\infty}\|_\infty<\gamma$

(3) Place the closed-loop poles in the region to guarantee some minimum decay rate $\alpha=-3$ and closed-loop damping 0.006, which satisfies some transient performance.

(4) Achieve these objectives for all possible values of the varying parameters. Since these parameters enter the plant state matrix in affine manner, we can model the parameter uncertainty by polytopic system with vertices corresponding to the combinations of extremal parameter values.

To solve Eq. (31), we have implemented a simplified continuation method involving the constraint constant γ (Bernstein and Haddad, 1989). The idea is to exploit the fact that for large γ the problem is approximated by H_2 which provides a reliable starting solution. The continuation parameter γ is then successively decreased until either a desired value of γ is achieved or no further decrease is possible. For trade off problems, H_∞ versus H_2 norm bound yields a trade-off curve as shown in Fig. 4.

In this curve we select the best compromise between the H_∞ and H_2 bounds. By inspection of this curve, the state-feedback gain K obtained for $\gamma=0.03$. Table 3 shows the pole locations of the open loop and closed loop system. Corresponding nominal and robust state feedback gains are $K_{nom}=[-44.61\ -112.69\ -573.72\ -4.72\ -5.70\ -11.59]$ and $K_{rob}=[-159.8\ -246.5\ -893.9\ -75.2\ -68.3\ -120.7]$.

Controller characteristics are given in Table 4. Moreover, in nominal case $\| T_{wz_\infty}\|_\infty=0.0153<\gamma=0.03$ and $\| T_{wz_2}\|=11.3608<trace(Y)=57.162$, which is acquired after 38 iterations. In robust case, $\| T_{wz_\infty}\|_\infty=0.0233<\gamma=0.03$ and $\| T_{wz_2}\|=11.3608<trace(Y)=60.344$, which is acquired after 70 iterations. The H_∞ and H_2 norms of the open loop system are $\| T_{wz_\infty}\|_\infty=0.608$ and $\| T_{wz_2}\|_2=63.015$, respectively.

A regional pole placement is applied to the piezo/beam system. The conic sector is located at

Table 3 Pole shifting due to control effect

Uncontrolled	Controlled
$-0.394\pm197.2j$	$-9.893\pm1147.82j$
$-2.296\pm1147.9j$	$-17.213\pm197.708j$
$-6.140\pm3070.0j$	$-22.021\pm3069.94j$

Table 4 $\| T_{wz}\|_\infty$ and $\| T_{wz}\|_2$ versus γ in nominal design

H_∞ norm bound γ	$\| T_{wz}\|_\infty$	H_2 norm bound Y	$\| T_{wz}\|_2$
0.01	0.0061	80.3019	16.3369
0.02	0.0116	62.6114	11.7606
0.03	0.0153	57.1623	11.3608
0.04	0.0169	54.9583	11.3366
0.05	0.0198	53.9380	11.2738
0.06	0.0220	53.3480	11 2177
0.07	0.0233	52.9872	11.1849

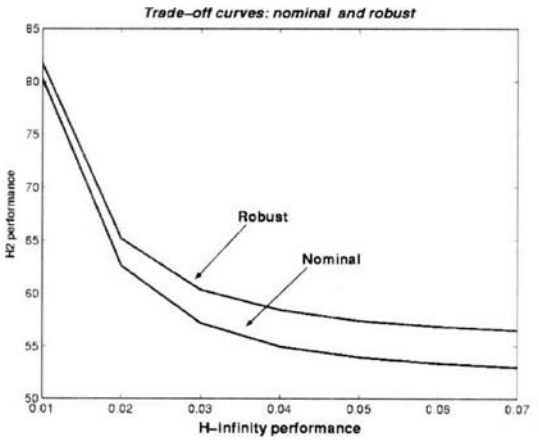

Fig. 4 Trade-off curve between the H_∞ and H_2 bound

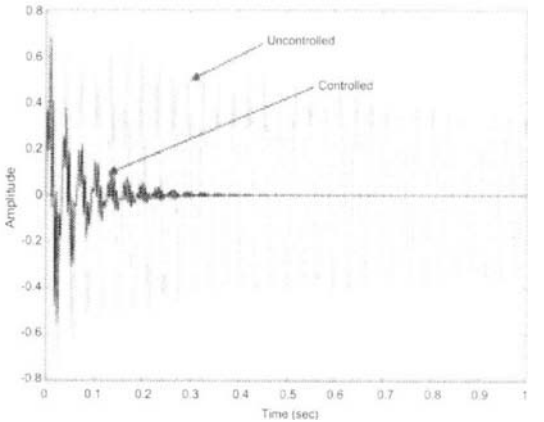

Fig. 5 Output system responses subject to impulse disturbance

the origin, which ensures to acquire a damping ratio $\zeta=0.02$.

Figure 5 displays the time response of the closed-loop system subject to impulse disturbances.

Figure 6 shows uncontrolled and controlled time response of the piezo/beam system subject to white noise excitations. For theses transient responses, the multiobjective state feedback control strategy is very effective in attenuating the settling time of the piezo/beam system.

Figure 7 superimposes the singular value plots with uncertainties that are $\pm 4\%$ range of natural frequency variations of the first mode.

The system is well operated to suppress the multiple modes over the broad frequency band.

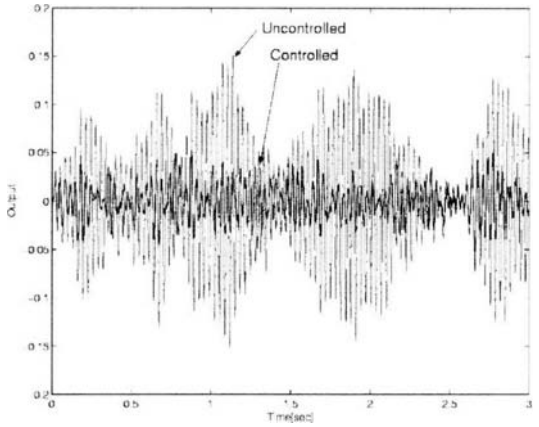

Fig. 6 Output system responses subject to random excitation

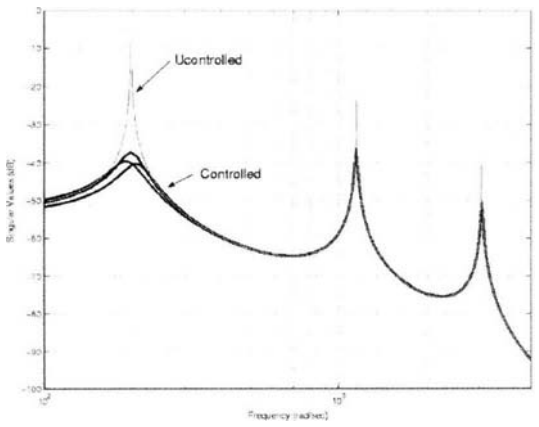

Fig. 7 Singular value plot for robust design (Uncertainties given at the first mode)

The vibration amplitudes are measured of 30dB reduction for the first mode, 13dB for the second mode, and 11dB for the third mode as shown in Fig. 7.

7. Conclusions

An integrated robust controller design procedure for a piezo/beam system with uncertainties due to natural frequency variation is presented in this paper. The design procedure involves the solutions of a multiobjective optimization problem involving different constraints on the controller. In the multiobjective state feedback controller, a systematic LMI based approach to mixed H_2/H_∞ synthesis with pole clustering constraints has been presented. For the theoretical analysis, the governing equation of motion of the smart structural system is derived by using Hamilton's principle. The effectiveness of an LMI based robust controller is demonstrated in damping out the multiple modes of vibration of the piezoelectric laminated beam subject to external disturbances and uncertainties.

References

Bailey, T. and Hubbard, J., 1985, "Distributed Piezoelectric Polymer Active Vibration Control of a Cantilever Beam," *Journal of Guidance, Control, and Dynamics*, Vol. 8, pp. 605~610.

Bernstein, D. S. and Haddad, W. M., "LQG Control with an Performance Bound : A Riccati Equation Approach," *IEEE Trans. on Automatic Control*, Vol. 34 (3), pp. 293~305.

Boyd, S., Ghaoui, L., Feron, E. and Balakrishnan, V., 1994 *Linear Matrix Inequalities in System and Control Theory*, SIAM.

Chilali, M. and Gahinet, P., 1996, "Desgin with Pole Placement Constraints : An LMI Approach," *IEEE Trans on Automatic Control*, Vol. 41 (3), pp. 358~369.

Fanson, J. L. and Caughey, T. K., 1990, "Positive Position Feedback Control for Large Space Structures," *AIAA Journal*, Vol. 28 (4), pp. 717~724.

Gahinet, P. and Apkarian, P., 1994, "A Linear

Matrix Inequality Approach to Control," *Int. J. of Robust and Nonlinear Control*, Vol. 4, pp. 421~448.

Gahinet, P., Nemirovski, L. and Chilali, M., 1995, *The LMI Control Toolbox*, Mathworks. Inc.

IEEE, 1987, *IEEE standard on piezoelectricity*, IEEE Std. 176-1987.

Khargonekar, P., Petersen, I. and Rotea, M., 1998, "H_∞-Optimal Control with State-Feedback," *IEEE Trans on Automatic Control*, Vol. 33, No. 8, pp. 786~788.

Kim, J. and Nam, C., 1996, "H_∞ Control for Flutter Suppression of a Laminated Plate with Self-Sensing Actuators," KSME Journal, Vol. 10 (2), pp. 169~179 in Korean.

Meirovitch, L., 1967, *Analytical Methods in Vibrations*, London : Macmillan.

Ogata, K., 1990, *Modern Control Engineering*, NJ : Prentice-Hall.

Petersen, I. R. 1987, "Disturbance Attenuation and Optimization : A Design Method Based on the Algebraic Riccati Equation," *IEEE Trans on Automatic Control*, Vol. 32, No. 5, pp. 427~429.

Rao, S. S., 1995, *Mechanical Vibrations*, Addison Wesley.

Scherer, C., Gahinet, P. and Chilali, M., 1997, "Multiobjective Output-Feedback Control via LMI Optimization," *IEEE Trans on Automatic Control*, Vol. 42, No. 7, pp. 896~911.

Shin, J., Hong, J., Park, S. and Oh, J., 1998, "Active Vibration Control of Flexible Cantilever Beam Using Piezo Actuator and Filtered-X LMS Algorithm," *KSME International Journal*, Vol. 12, No. 4, pp. 665~671.